

Transient receptor potential melastatin 3 is a phosphoinositide-dependent ion channel

Doreen Badheka, Istvan Borbiri, and Tibor Rohacs

Department of Pharmacology and Physiology, Rutgers New Jersey Medical School, Newark, NJ 07103

Phosphoinositides are emerging as general regulators of the functionally diverse transient receptor potential (TRP) ion channel family. Phosphatidylinositol 4,5-bisphosphate (PI(4,5)P₂) has been reported to positively regulate many TRP channels, but in several cases phosphoinositide regulation is controversial. TRP melastatin 3 (TRPM3) is a heat-activated ion channel that is also stimulated by chemical agonists, such as pregnenolone sulfate. Here, we used a wide array of approaches to determine the effects of phosphoinositides on TRPM3. We found that channel activity in excised inside-out patches decreased over time (rundown), an attribute of PI(4,5)P₂-dependent ion channels. Channel activity could be restored by application of either synthetic dioctanoyl (diC₈) or natural arachidonyl stearyl (AASt) PI(4,5)P₂. The PI(4,5)P₂ precursor phosphatidylinositol 4-phosphate (PI(4)P) was less effective at restoring channel activity. TRPM3 currents were also restored by MgATP, an effect which was inhibited by two different phosphatidylinositol 4-kinase inhibitors, or by pretreatment with a phosphatidylinositol-specific phospholipase C (PI-PLC) enzyme, indicating that MgATP acted by generating phosphoinositides. In intact cells, reduction of PI(4,5)P₂ levels by chemically inducible phosphoinositide phosphatases or a voltage-sensitive 5'-phosphatase inhibited channel activity. Activation of PLC via muscarinic receptors also inhibited TRPM3 channel activity. Overall, our data indicate that TRPM3 is a phosphoinositide-dependent ion channel and that decreasing PI(4,5)P₂ abundance limits its activity. As all other members of the TRPM family have also been shown to require PI(4,5)P₂ for activity, our data establish PI(4,5)P₂ as a general positive cofactor of this ion channel subfamily.

INTRODUCTION

Transient receptor potential (TRP) melastatin 3 (TRPM3) is a member of the TRP ion channel family. It is expressed in several different tissues, including the kidneys, eyes, sensory neurons of the dorsal root ganglia, and pancreatic β cells (Oberwinkler and Philipp, 2014). TRPM3 has been proposed to play roles in a variety of physiological and pathophysiological processes. It is activated by high temperatures and was shown to function as a noxious heat sensor in dorsal root ganglion neurons (Vriens et al., 2011). The neurosteroid pregnenolone sulfate (PregS) activates TRPM3 in pancreatic β cells (Wagner et al., 2008), and the channel has been proposed to play important signaling roles in those cells (Thiel et al., 2013). A missense mutation in TRPM3 was recently shown to underlie inherited cataract and high-tension glaucoma in humans (Bennett et al., 2014). In mice, genetic deletion of TRPM3 caused impaired pupillary light reflexes (Hughes et al., 2012).

TRP channels are activated by a wide range of stimuli and play roles in a variety of physiological and pathophysiological processes (Wu et al., 2010). Given their diversity, general principles in their regulation are difficult to establish. As the majority of TRP channels have been reported to be regulated by phosphatidylinositol 4,5-bisphosphate (PI(4,5)P₂), it is possible that phosphoinositides are general regulators of all TRP channels.

PI(4,5)P₂ regulates many different mammalian ion channels. It usually acts as a positive cofactor; for example, its presence is required for the activity of all members of the K⁺ inwardly rectifying (Kir) and KCNQ K⁺ channel families (Suh and Hille, 2008; Logothetis et al., 2015). In contrast, PI(4,5)P₂ regulation of TRP channels is complex; both positive and negative effects of this lipid have been demonstrated on several members of the TRP vanilloid (TRPV) and TRP classical (TRPC) families (Rohacs, 2014). In contrast, the picture on the TRPM family is simpler. Six of the eight mammalian TRPM channels, TRPM2 (Tóth and Csanády, 2012), TRPM4 (Nilius et al., 2006), TRPM5 (Liu and Liman, 2003), TRPM6 (Xie et al., 2011), TRPM7 (Runnels et al., 2002), and TRPM8 (Rohács et al., 2005), have been shown to be positively regulated by PI(4,5)P₂, and

Correspondence to Tibor Rohacs: rohacsti@njms.rutgers.edu

Abbreviations used in this paper: AASt, arachidonyl stearyl; ci-VSP, voltage-sensitive phosphatase from *Ciona intestinalis*; diC₈, dioctanoyl; Kir, K⁺ inwardly rectifying; Kv, voltage-gated K⁺; PI(3,4,5)P₃, phosphatidylinositol 3,4,5-trisphosphate; PI3K, phosphoinositide 3-kinase; PI(4,5)P₂, phosphatidylinositol 4,5-bisphosphate; PI4K, phosphatidylinositol 4-kinase; PI(4)P, phosphatidylinositol 4-phosphate; PI-PLC, phosphatidylinositol-specific PLC; Poly-Lys, poly-L-lysine; PregS, pregnenolone sulfate; TEVC, two-electrode voltage clamp; TRP, transient receptor potential; TRPM, TRP melastatin; TRPV, TRP vanilloid.

© 2015 Badheka et al. This article is distributed under the terms of an Attribution-Noncommercial-Share Alike-No Mirror Sites license for the first six months after the publication date (see <http://www.rupress.org/terms>). After six months it is available under a Creative Commons License (Attribution-Noncommercial-Share Alike 3.0 Unported license, as described at <http://creativecommons.org/licenses/by-nc-sa/3.0/>).

no negative effect of the lipid has been reported on any TRPM channel (Rohacs, 2014).

Here we set out to test the effects of PI(4,5)P₂ on TRPM3. One of our motivations was to assess whether PI(4,5)P₂ is a general positive regulator of the TRPM family. TRPM1 is very difficult to study in expression systems; thus, the only remaining member of the TRPM family on which functional effects of PI(4,5)P₂ are reliably testable, but has not been demonstrated yet, is TRPM3. We used an array of approaches that included testing endogenous and exogenous phosphoinositides in excised inside-out patches and various inducible phosphatases in whole-cell patch clamp experiments. All of these techniques point to the same conclusion: PI(4,5)P₂ is required for TRPM3 activity. Overall, our work establishes that PI(4,5)P₂ is an important cofactor for TRPM3 and, together with data in the literature, suggests that PI(4,5)P₂ is a general positive regulator of the TRPM family.

MATERIALS AND METHODS

Xenopus laevis oocyte preparation

Xenopus oocytes were prepared as described earlier (Rohacs, 2013). In brief, frogs were anesthetized in 0.25% ethyl 3-aminobenzoate methanesulfonate solution (MS222; Sigma-Aldrich) in H₂O, pH 7.4. Bags of ovaries containing multiple oocytes were removed surgically from the anesthetized frogs. Individual oocytes were obtained by overnight digestion at 16°C in 0.1–0.2 mg/ml type 1A collagenase (Sigma-Aldrich), dissolved in a solution containing 82.5 mM NaCl, 2 mM KCl, 1 mM MgCl₂, and 5 mM HEPES, pH 7.4 (OR₂ solution). The next day the collagenase-containing solution was discarded and the oocytes were washed multiple times with OR₂ solution. The oocytes were maintained in OR₂ solution supplemented with 1.8 mM CaCl₂, 100 IU/ml penicillin, and 100 µg/ml streptomycin at 16°C. 40 ng linearized cRNA transcribed from the human TRPM3 (hTRPM3) cDNA clone (Grimm et al., 2003) in the pGEMSH vector was microinjected into individual oocytes. The injection was performed with a nanoliter-injector system (Warner Instruments). Oocytes were used for electrophysiological measurements 48–72 h after microinjection. The hTRPM3 clone in a mammalian expression vector was provided by C. Harteneck (Eberhard Karls University Tübingen, Tübingen, Germany). The cDNA of hTRPM3 was subcloned into pGEMSH using standard molecular biology techniques.

Excised inside-out patch clamp and two-electrode voltage clamp (TEVC) electrophysiology

Excised inside-out patch clamp measurements were performed as described earlier (Rohacs, 2013). In brief, oocytes were placed in bath solution (97 mM KCl, 5 mM EGTA, and 10 mM HEPES, pH 7.4) in the recording chamber. The vitelline layer was manually removed with a pair of forceps, and then gigaohm seals were formed with borosilicate glass pipettes (World Precision Instruments) containing pipette solution (97 mM NaCl, 2 mM KCl, 1 mM MgCl₂, 5 mM HEPES, and 100 µM PregS, pH 7.4). Pipette resistance was 0.8–1 MΩ. Macroscopic currents were recorded with a –100- to 100-mV ramp protocol applied every second (0.25 mV/ms); holding potential was 0 mV. The currents were measured with an Axopatch 200B amplifier and analyzed with the pClamp 9.0 software (Molecular Devices). Once the excised

inside-out patch configuration was established, the test compounds, dissolved in bath solution, were applied through a custom-made perfusion system to the cytoplasmic face of the membrane patch. The dioctanoyl (diC₈) forms of phosphoinositides, phosphatidylinositol 4-phosphate (PI(4)P), PI(3,4)P₂, PI(4,5)P₂, PI(3,5)P₂, and phosphatidylinositol 3,4,5-trisphosphate (PI(3,4,5)P₃), were purchased from Cayman Chemicals. The naturally occurring arachidonyl stearyl (AASt) forms of PI(4)P and PI(4,5)P₂, purified from porcine brain, were purchased from Avanti Polar Lipids, Inc., and they were sonicated on ice for 10 min before experiments with an ultrasonic homogenizer (model 3000 V/T; Biologics Inc.). All phosphoinositides were dissolved in water, aliquoted, and stored at –80°C. Poly-L-lysine (Poly-Lys; molecular mass 4–15 kD), LY294002, PregS, and Gö6976 were purchased from Sigma-Aldrich, dissolved in DMSO, and stored at –20°C. LY294002 was added into the MgATP solution from a 100 mM stock, and DMSO was used in control recordings at the same final concentration (0.3%). The concentration of DMSO for PregS-containing solutions did not exceed 0.2%. Phosphatidylinositol-specific PLC (PI-PLC) was purchased from Sigma-Aldrich as a glycerol-containing stock solution and stored at 4°C; glycerol (0.5%) was added to control solutions in experiments with PI-PLC. Compound A1, provided by T. Balla (National Institutes of Health, Bethesda, MD; Bojjireddy et al., 2014), was dissolved in DMSO. For the MgATP experiments, the pH of the bath solution had to be readjusted to pH 7.4; for details see Zakharian et al. (2011).

Data analysis for inside-out patch clamp. In Fig. 1, data have been normalized to the peak current immediately after excision. In the remaining figures, the responses have been normalized to the current induced by the 25 µM diC₈ PI(4,5)P₂ applied after the current had run down. For the dose–response measurements in Figs. 1 and 2, repetitive pulses of 25 µM diC₈ PI(4,5)P₂ were applied to compensate for any decrease in responsiveness of the patch. Amplitudes evoked by different concentrations of either diC₈ PI(4,5)P₂ or PI(3,4,5)P₃ were normalized to the mean of the amplitudes evoked by the two nearest 25 µM diC₈ PI(4,5)P₂ applications. Data were then fitted with the Hill equation, using the Origin 9.0 software. For plotting the data in the figures, data points were renormalized to the maximal current obtained from the Hill fits.

TEVC measurements were performed as described earlier (Lukacs et al., 2007); in brief, oocytes were placed in extracellular solution (97 mM NaCl, 2 mM KCl, 1 mM MgCl₂, and 5 mM HEPES, pH 7.4), and currents were recorded with thin-wall inner-filament-containing glass pipettes (World Precision Instruments) filled with 3 M KCl in 1% agarose. Currents were measured with the same ramp protocol as mentioned above for excised inside-out patch measurements. For experiments with wortmannin, oocytes were pretested for PregS-induced TRPM3 currents and then incubated for 2 h in wortmannin-containing OR₂ solution. PregS-induced TRPM3 currents were measured again, and the currents before and after wortmannin incubation were compared in the same oocytes. The currents were recorded with a GeneClamp 500B amplifier and analyzed with the pClamp 9.0 software (Molecular Devices).

Whole-cell electrophysiology in HEK cells

Whole-cell patch clamp measurements were performed in Human Embryonic Kidney 293 (HEK293) cells (ATCC) transiently transfected using the Effectene reagent (QIAGEN), with the mouse TRPM3α2 (mTRPM3α2) cloned in the bicistronic pCAGGS/IRES-GFP vector (Oberwinkler et al., 2005; Vriens et al., 2011), provided by S. Philipp and V. Flockerzi (Saarland University, Homburg, Germany). The cells were maintained in MEM (Life Technologies) supplemented with 10% (vol/vol) fetal bovine

serum, 100 IU/ml penicillin, and 100 µg/ml streptomycin. GFP-positive cells were used for measurements. For the experiments with the voltage-sensitive phosphatase from *Ciona intestinalis* (ci-VSP), the cells were cotransfected with ci-VSP in the pIRES2-GFP vector (Hossain et al., 2008), provided by Y. Okamura (Osaka University, Suita, Osaka, Japan) and Kir2.1 in pCDNA3 vector to keep the membrane potential in the negative range to avoid any basal activation of the phosphatase. The cells were used for measurements 48–72 h after transfection. Measurements were performed in an extracellular solution containing 137 mM NaCl, 5 mM KCl, 1 mM MgCl₂, 10 mM HEPES, and 10 mM glucose, pH 7.4. For measurements in Fig. 7, the same solution was supplemented with 0.5 mM EGTA, and for Fig. 8, the solution was supplemented with 2 mM CaCl₂. The recording pipette was filled with intracellular solution containing 140 mM potassium gluconate, 5 mM EGTA, 1 mM MgCl₂, 10 mM HEPES, and 2 mM Na-ATP, pH 7.3, adjusted with KOH. For experiments in Fig. 8, this solution was supplemented with 0.2 mM GTP. Once a gigaohm seal was achieved, the whole-cell configuration was established, and the currents were recorded at a constant holding potential of –100 mV. To activate ci-VSP, a 5-s pulse to 100 mV was applied. For measurements with the various rapamycin-inducible phosphatases, cells were cotransfected with mTRPM3α2 and the components of either the rapamycin-inducible 5'-phosphatase (Varnai et al., 2006), provided by T. Balla (National Institutes of Health, Bethesda, MD), or pseudojanin (Hammond et al., 2012), provided by G. Hammond (University of Pittsburgh, Pittsburgh, PA). Experiments were performed with a ramp protocol from –100 to 100 mV applied once every second, and the currents at –100 and 100 mV were plotted. The currents were measured with an Axopatch 200B amplifier, filtered at 2 kHz, digitized through Digidata 1322A, and analyzed with pCLAMP 9.0 software (Molecular Devices).

Statistics

Statistical analysis was performed using Student's *t* test or analysis of variance: *, *P* < 0.05; **, *P* < 0.01; ***, *P* < 0.005. The error bars in all of the figures represent SEM.

Online supplemental material

Fig. S1 shows that PregS activates hTRPM3 expressed in *Xenopus* oocytes in a concentration-dependent manner. Fig. S2 shows that intracellular Mg²⁺ inhibits hTRPM3 after patch excision. Fig. S3 shows that intracellular Mg²⁺ inhibits the current increase after washout of MgATP in excised patches and Poly-Lys inhibits MgATP-induced currents in excised patches. Fig. S4 shows that the PKC inhibitor Gö6976 does not inhibit the effect of MgATP in excised patches. Fig. S5 shows that the rapamycin-inducible 5'-phosphatase inhibits hTRPM3 expressed in *Xenopus* oocytes. Online supplemental material is available at <http://www.jgp.org/cgi/content/full/jgp.201411336/DC1>.

RESULTS

Exogenous phosphoinositides reactivate TRPM3 currents in excised patches after current rundown

The neurosteroid PregS is a well-established activator of TRPM3. Both the human and the mouse TRPM3 have several splice variants, summarized in Oberwinkler et al. (2005). Most experiments documenting the activating effect of PregS on TRPM3 have been performed on the α2 isoform of the mouse TRPM3 (mTRPM3α2; Wagner et al., 2008; Vriens et al., 2011; Frühwald et al., 2012). Here we used the isoform of the human TRPM3 (hTRPM3)

described in Grimm et al. (2003) for electrophysiological recordings in *Xenopus* oocytes. First we tested whether PregS is a reliable activator of hTRPM3 in TEVC experiments. We found that PregS induced outwardly rectifying currents in TRPM3-expressing oocytes in a concentration-dependent manner, with an EC₅₀ of 19.3 µM at 100 mV and 28.5 µM at –100 mV (Fig. S1).

Our central hypothesis is that PI(4,5)P₂ is required for the activity of TRPM3. PI(4,5)P₂ is found in the inner leaflet of the plasma membrane; thus, we tested the effects of phosphoinositides applied directly to the cytoplasmic side of excised inside-out patches. In the cell-attached configuration, with 100 µM PregS in the patch pipette, hTRPM3 currents were relatively small, and they increased substantially immediately after excision (Fig. 1, A–C and E), reflecting the loss of a cytoplasmic inhibitory factor. Intracellular Mg²⁺ ions inhibit TRPM3 (Oberwinkler et al., 2005). Intracellular free Mg²⁺ concentrations in *Xenopus* oocytes were reported to be ~0.3 mM (Gabriel and Günzel, 2007), which is within the range of that in most mammalian cell types (0.25–1 mM; Grubbs, 2002). To test whether current amplitudes increase after excision into the Mg²⁺ free bath solution because of the loss of Mg²⁺, we also excised patches into a bath solution containing 0.3 and 1 mM Mg²⁺. As shown in Fig. S2, the increase after excision was somewhat smaller in 0.3 mM Mg²⁺ than in 0 Mg²⁺, and no increase was detected when the patch was excised into 1 mM Mg²⁺. These data suggest that relief from Mg²⁺ inhibition contributes to the current increase but is unlikely to be solely responsible for it.

After the current had reached the peak, it decreased (rundown) to <10% of the initial current within 2–5 min in most patches at 100 mV. In some patches rundown was slower, but even there current amplitudes decreased to 10–20% of the original current level. Current rundown at –100 mV was generally more complete, usually reaching zero. At negative voltages, however, reliable differentiation from leak was not always possible because of the small current amplitudes; thus, most statistical analysis was performed for excised patch measurements at 100 mV. Nevertheless, we show the inward currents in the figures because those are the physiologically relevant currents for nonselective cation channels. Rundown in excised inside-out patches generally is caused by the loss of a positive cofactor when the patch is removed from the cellular environment. In many cases, the lost cofactor is PI(4,5)P₂, which is dephosphorylated by endogenous phosphoinositide phosphatases in the patch membrane (Hilgemann, 1997).

To test whether PI(4,5)P₂ is the lost cofactor for TRPM3, we perfused excised inside-out patches with various phosphoinositides after the current had run down. As shown in Fig. 1 (A and D), application of the natural long acyl chain AAsT PI(4,5)P₂ (10 µM) restored the TRPM3 currents to levels higher than those immediately after excision. The effect developed slowly; the

time to reach 50% of the effect was 96 ± 18 s. This slow effect is consistent with the slow incorporation of long acyl chain PI(4,5)P₂ micelles in the membrane (Rohács et al., 2002). Stimulation of PI(4,5)P₂-sensitive ion channels by AAST PI(4,5)P₂ is generally not reversible on the 2–5-min time scale (Rohács et al., 2002; Zakharian et al., 2011), but can be inhibited by Poly-Lys, a known chelator of phosphoinositides and other negatively charged lipids (Lopes et al., 2002). We found that 30 μ g/ml Poly-Lys decreased the TRPM3 currents close to baseline level after AAST PI(4,5)P₂ (Fig. 1, A and D). PI(4)P, the precursor of PI(4,5)P₂, is found in the plasma membrane at similar quantities to PI(4,5)P₂ and may also activate ion channels such as TRPV1 (Lukacs et al., 2007; Klein et al., 2008; Ufret-Vincenty et al., 2011). AAST PI(4)P increased the TRPM3 current to a smaller extent compared with AAST PI(4,5)P₂ (Fig. 1, B and D). The effect developed slowly, with a similar kinetics to AAST PI(4,5)P₂; the time to reach 50% of the effect for AAST PI(4)P was 114 ± 12 s.

We also tested the effects of the synthetic diC₈ PI(4,5)P₂ and PI(4)P. These short acyl chain water-soluble phosphoinositide analogues are routinely used to study ion channel regulation because their effective concentrations

can be easily controlled and their effects are readily reversible (Rohács et al., 2002; Nilius et al., 2006; Stein et al., 2006). As shown in Fig. 1 (A–D), application of diC₈ PI(4,5)P₂ stimulated TRPM3 currents after rundown in a quickly reversible fashion, whereas 25 μ M diC₈ PI(4)P only had a marginal effect (Fig. 1, C and D). DiC₈ PI(4,5)P₂ reliably stimulated TRPM3 currents in the same patches, both before and after the application of PI(4)P, showing that the lack of effect of the latter was not caused by the lack of responsiveness of the patch. We also determined the concentration dependence of the effect of diC₈ PI(4,5)P₂ by applying the lipid consecutively at different concentrations to the same patch. PI(4,5)P₂ stimulated TRPM3 activity with an EC₅₀ of 18 μ M (Fig. 1, E and F). Note that the effect of diC₈ PI(4,5)P₂ was smaller than that of AAST PI(4,5)P₂ (Fig. 1 D), even at the highest concentration tested (100 μ M; Fig. 1 F).

We also tested whether other phosphoinositides can stimulate TRPM3. Fig. 2 (A–D) shows that 25 μ M diC₈ PI(3,4)P₂, PI(3,4,5)P₃, and PI(3,5)P₂ also activated TRPM3 after current rundown. At this concentration PI(3,4)P₂ was slightly less active than PI(4,5)P₂, PI(3,5)P₂ was somewhat more active, and PI(3,4,5)P₃ had the highest activity. We tested the concentration dependence of

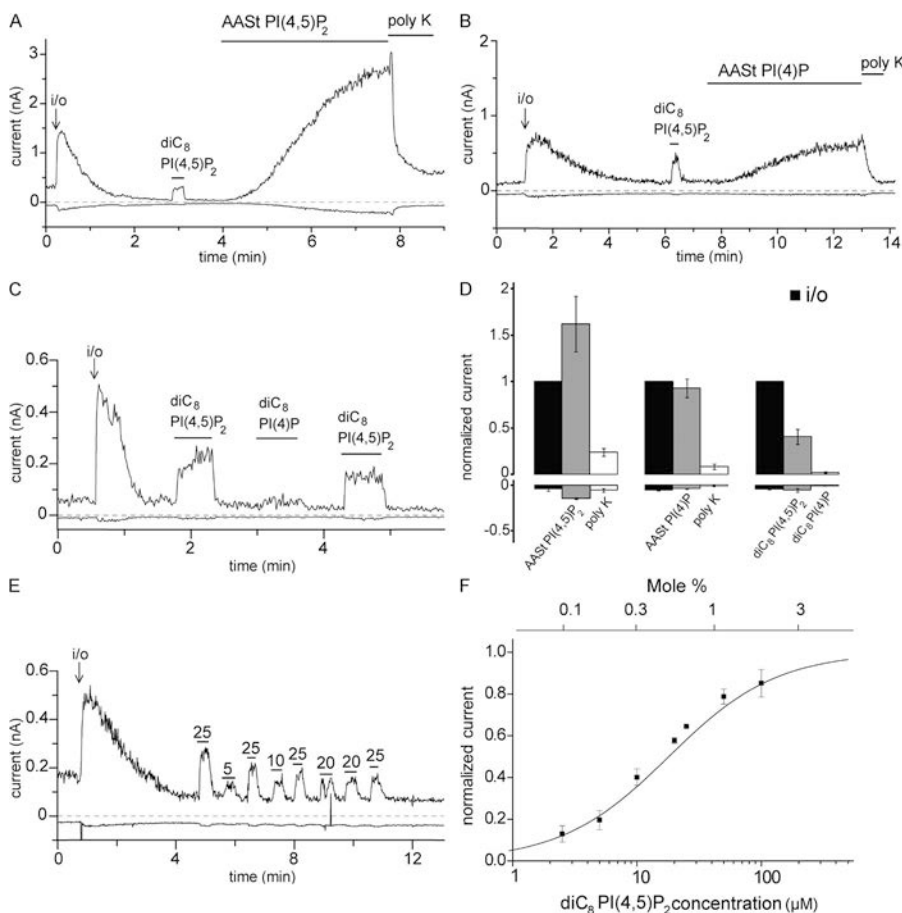


Figure 1. PI(4,5)P₂ reactivates hTRPM3 in excised inside-out patches after rundown. (A–C) Representative traces at 100 and –100 mV; experiments were performed on hTRPM3-expressing *Xenopus* oocytes with 100 μ M PregS in the patch pipette as described in Materials and methods. The measurements start in the cell-attached mode; the establishment of the inside-out configuration (i/o) is indicated with an arrow. (D) Statistical summary; the data are normalized to the TRPM3 current immediately after the establishment of the inside-out configuration at 100 mV ($n = 6–7$). (E) Representative trace showing the effects of different concentrations (μ M) of diC₈ PI(4,5)P₂ applied to an excised inside-out patch; 25 μ M diC₈ PI(4,5)P₂ was applied repetitively to normalize the effect of other concentrations and control for any time-dependent decrease in the responsiveness of TRPM3. (F) Summary of the dose–response relationship of diC₈ PI(4,5)P₂ ($n = 4–10$ for the individual concentrations), EC₅₀ = 18.01 μ M. Current values were initially normalized to the effect of the repetitively applied 25 μ M diC₈ PI(4,5)P₂ and then renormalized for plotting

to the maximal value obtained by the curve fitting. The top horizontal axis shows the mole percentage corresponding to the diC₈ PI(4,5)P₂ concentrations calculated using the formula from Collins and Gordon (2013). Error bars represent SEM.

the effect of PI(3,4,5)P₃ in patches, where we also applied 25 μM diC₈ PI(4,5)P₂ as a normalizing stimulus to make the results quantitatively comparable with those obtained with diC₈ PI(4,5)P₂ (Fig. 2, E and F). Based on the Hill fits, PI(3,4,5)P₃ had an approximately twofold higher maximal activity and a left-shifted concentration dependence (EC₅₀ = 9.4 μM) when compared with PI(4,5)P₂ (Fig. 2, E and F).

In addition to the marked rundown of current activity after excision, we also observed a moderate reduction in responsiveness to diC₈ PI(4,5)P₂ in many, but not all, patches. We quantitated this phenomenon in 13 patches where diC₈ PI(4,5)P₂ was applied at least four times. In those patches, on average, the second pulse of diC₈ PI(4,5)P₂ gave 82 ± 6% of the response evoked by the first application. The third and fourth applications gave 67 ± 8% and 66 ± 9% of the first response, respectively. This reduced responsiveness is a relatively small effect compared with the almost complete rundown even by the first application of diC₈ PI(4,5)P₂, and we did not further examine its mechanism. Similar phenomena have been observed with many well-established PI(4,5)P₂-dependent ion channels, for example Kir2.1 (Rohács et al., 2003), TRPM8 (Rohács et al., 2005), and TRPV6 (Cao et al., 2013a).

The effects of endogenous PI(4,5)P₂ in excised inside-out patches

Our data so far show that exogenously applied PI(4,5)P₂ and other phosphoinositides stimulate TRPM3 after

current rundown. However, exogenous lipophilic molecules can potentially cause membrane perturbations (Hilgemann, 2012; Ingólfsson et al., 2014); thus, we also tested whether endogenous PI(4,5)P₂ would have a similar effect. PI(4,5)P₂ can be replenished by perfusing excised membrane patches with MgATP, which is required for the activity of phosphoinositide kinases in the patch membrane (Hilgemann and Ball, 1996; Sui et al., 1998; Zakharian et al., 2011). As shown in Fig. 3 A, application of 2 mM MgATP increased TRPM3 currents slowly. Upon washout of MgATP, current amplitudes increased transiently, followed by a slow decrease. The peak of the transiently increased current was measured as MgATP-activated TRPM3 current for statistical analysis. Free Mg²⁺ in the MgATP solution was calculated to be 0.3 mM using the MaxChelator program. When the MgATP solution was switched to bath solution containing 0.3 mM Mg²⁺, the current increase was not observed, signifying that it was caused by relief from inhibition by Mg²⁺ (Fig. S3 A). The slow decrease in current after the peak is likely caused by dephosphorylation of PI(4,5)P₂ and PI(4)P by lipid phosphatases in the patch, similar to that observed during rundown after patch excision.

PI(4,5)P₂ is generated from phosphatidylinositol by the sequential action of phosphatidylinositol 4-kinases (PI4Ks) and PI(4)P 5-kinases (PIP5Ks; Balla, 2013). PI(4,5)P₂ can be further phosphorylated to PI(3,4,5)P₃ upon activation of phosphoinositide 3-kinases (PI3Ks). To demonstrate that MgATP stimulated TRPM3 currents through increased production of PI(4,5)P₂, we tested the

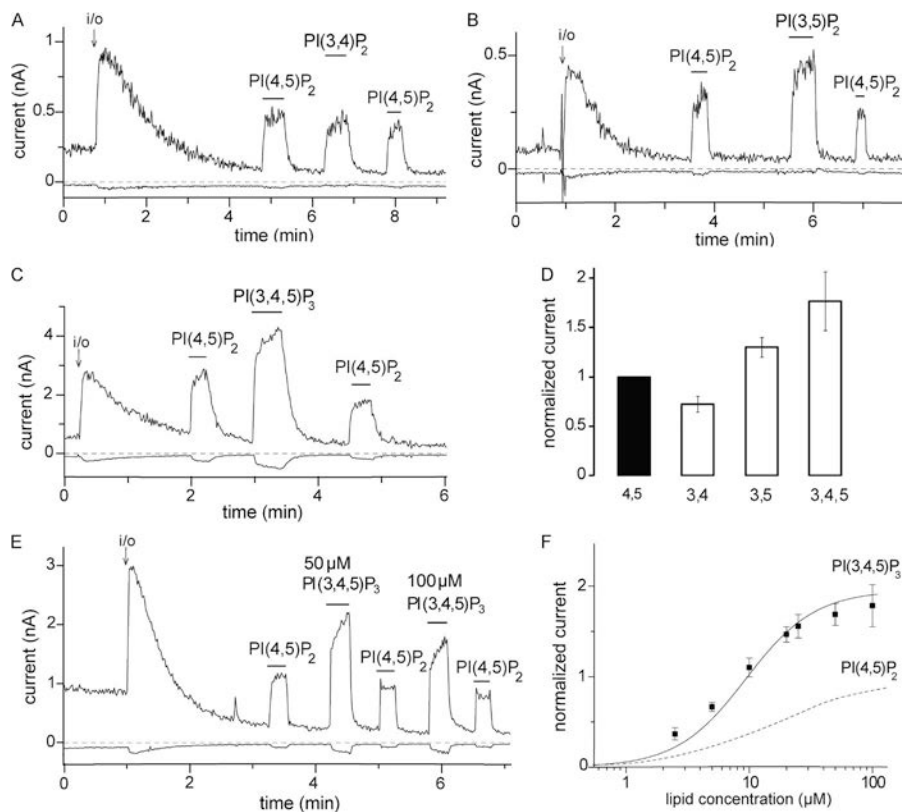


Figure 2. The effects of 3-phosphorylated phosphoinositides on hTRPM3. (A–C) Representative traces at 100 and –100 mV; experiments were performed on hTRPM3-expressing *Xenopus* oocytes with 100 μM PregS in the patch pipette as described in Materials and methods. The establishment of the inside-out (i/o) configuration is indicated with an arrow. The applications of 25 μM diC₈ PI(4,5)P₂, 25 μM diC₈ PI(3,4)P₂, 25 μM diC₈ PI(3,5)P₂, and 25 μM diC₈ PI(3,4,5)P₃ are indicated with the horizontal lines. (D) Statistical summary of current amplitudes at 100 mV; the data are normalized to the TRPM3 current evoked by diC₈ PI(4,5)P₂ ($n = 6–7$). (E) Representative measurement for a concentration–response relationship for PI(3,4,5)P₃. (F) Statistical summary compared with PI(4,5)P₂, which is replotted from Fig. 1 F (dashed line). Error bars represent SEM.

effects of MgATP in the presence of LY294002. This compound is known to inhibit PI3Ks at low micromolar concentrations and type III PI4Ks (PI4KA and PI4KB) at high micromolar concentrations (Balla, 2001). When 300 μM LY294002 was applied along with MgATP, the ability of MgATP to reactivate TRPM3 currents was lost (Fig. 3 B). The effect of MgATP was not inhibited by 10 μM LY294002 (Fig. 3 C), indicating that 300 μM LY294002 inhibited the TRPM3 currents via inhibiting PI4K. When Poly-Lys was applied after MgATP, it quickly inhibited TRPM3 currents (Fig. S3, C and D), again suggesting that MgATP acted via generating PI(4,5)P₂.

Recently, novel, more potent, and more specific PI4K inhibitors became available (Bojjireddy et al., 2014). We tested one of these novel compounds (A1), which inhibits PI3K enzymes at higher concentrations than PI4K and shows preference for the PI4KA enzymes over PI4KB. As shown in Fig. 3 (D–F), compound A1 completely inhibited the effect of MgATP at 100 nM and exerted an $\sim 70\%$ inhibition at 10 nM. The IC₅₀ of A1 was reported to be ~ 50 nM for PI3K, but 0.15 or 3.1 nM for PI4KA and 19 and 63 nM for PI4KB in two different assays (Bojjireddy et al., 2014). Given the $\sim 70\%$ inhibition of the effect of MgATP at 10 nM, it is likely that MgATP exerted its effect predominantly via PI4KA. However, a firm conclusion is difficult to draw because the pharmacological profile of *Xenopus* PI4K enzymes is not known.

In addition to pharmacological inhibitors, we also used a bacterial PI-PLC, which selectively hydrolyses phosphatidylinositol, thus removing the precursor for PI(4)P and PI(4,5)P₂ (Hilgemann and Ball, 1996; Sui et al., 1998). Pretreatment with PI-PLC almost completely

prevented the effect of MgATP, showing again that the latter acted via generating phosphoinositides (Fig. 4). MgATP is also a cofactor for protein kinases; thus, we also tested the effect of a PKC inhibitor. Fig. S4 shows that 1 μM Gö6976 did not inhibit the effect of MgATP. Collectively, our data suggest that endogenous PI(4,5)P₂ is important for the activity of TRPM3.

Inhibition of PI4K inhibits TRPM3 currents in intact cells

Next we tested whether reducing the concentration of PI(4,5)P₂ in intact cells limits TRPM3 activity. In these experiments, we used another inhibitor of type III PI4 kinases, wortmannin. Wortmannin inhibits PI3K at low nanomolar concentrations and type III PI4 kinases at micromolar concentrations. We recorded PregS-induced currents from *Xenopus* oocytes expressing hTRPM3 in TEVC experiments (Fig. 5 A). After measuring TRPM3 currents, the oocytes were incubated in either 35 nM or 35 μM wortmannin for 2 h, and then the PregS-induced currents were measured again in the same oocytes. As shown in Fig. 5 (B and C), current amplitudes decreased significantly in oocytes incubated in 35 μM wortmannin, but not in oocytes incubated in 35 nM wortmannin, showing that the effect is caused by inhibition of type III PI4Ks, indicating that PI(4,5)P₂ is vital for the optimal functioning of TRPM3.

TRPM3 currents are inhibited by rapidly inducible phosphoinositide phosphatases

All of our experiments so far were performed in oocytes heterologously expressing hTRPM3. However, most of the studies on TRPM3 used the mTRPM3 $\alpha 2$ clone. To

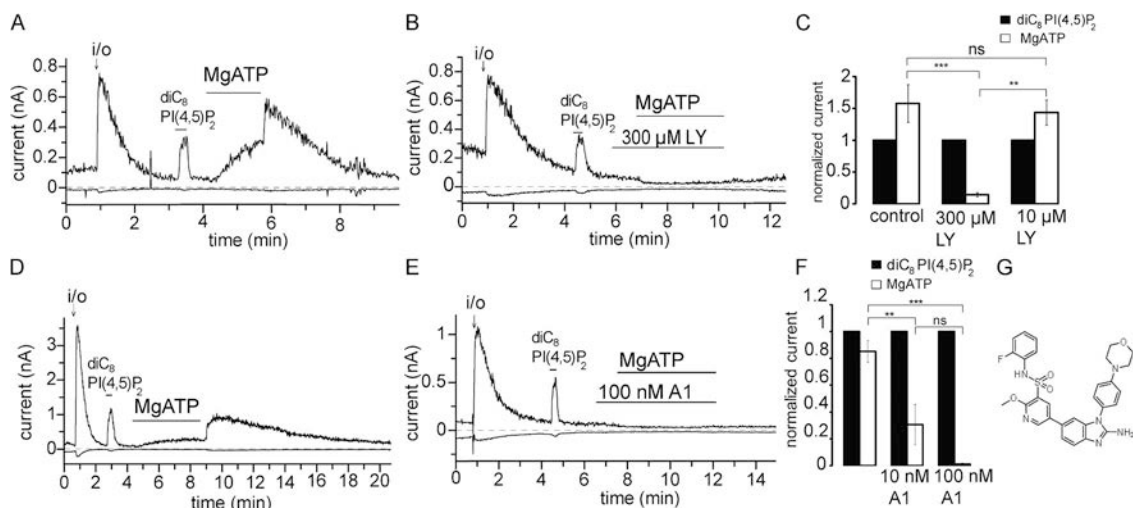


Figure 3. MgATP reactivates hTRPM3 through PI4Ks. Excised inside-out patch measurements have been performed on TRPM3-expressing *Xenopus* oocytes with 100 μM PregS in the patch pipette as described in Materials and methods; data are plotted at 100 and -100 mV. (A and B) Representative traces for the effects of MgATP in the absence and presence of LY294002 (LY); the applications of 2 mM MgATP, 300 μM LY294002, and 25 μM diC₈ PI(4,5)P₂ are indicated by the horizontal lines. (C) Summary of the data for control and 10 and 100 μM LY294002 ($n = 5$ for control and 300 μM LY and $n = 3$ for 10 nM LY). (D and E) Representative traces for the effects of MgATP in the absence and presence of the PI4K inhibitor A1; the applications of 2 mM MgATP 100 nM A1 and 25 μM diC₈ PI(4,5)P₂ are indicated by the horizontal lines. (F) Summary of the data for control and 10 and 100 nM A1 ($n = 5-6$). (G) Chemical formula for compound A1. Error bars represent SEM. **, $P < 0.01$; ***, $P < 0.005$.

test whether PI(4,5)P₂ is also necessary for the function of mTRPM3α2, we expressed these channels in HEK293 cells and studied the effects of various inducible phosphoinositide phosphatases on channel activity. The experiments were performed in the absence of extracellular Ca²⁺ to avoid desensitization of PregS-induced TRPM3 currents (see last paragraph of Results). First, we depleted membrane PI(4,5)P₂ using ci-VSP. At negative voltages (−100 mV), ci-VSP is inactive, probably because its phosphatase domain is located away from the cell membrane. When the cell is depolarized, the phosphatase is activated and dephosphorylates PI(4,5)P₂ to PI(4)P (Okamura et al., 2009). To test the effect of ci-VSP activation on TRPM3, we recorded PregS-induced TRPM3 currents from HEK cells in the whole-cell configuration at a holding potential of −100 mV, where ci-VSP is inactive. In the presence of PregS, the membrane was depolarized with a short pulse (5 s) of 100 mV to activate the phosphatase, and then potential was returned to −100 mV. As shown in Fig. 6 A, upon activation of ci-VSP by depolarization, PregS-induced TRPM3 currents were

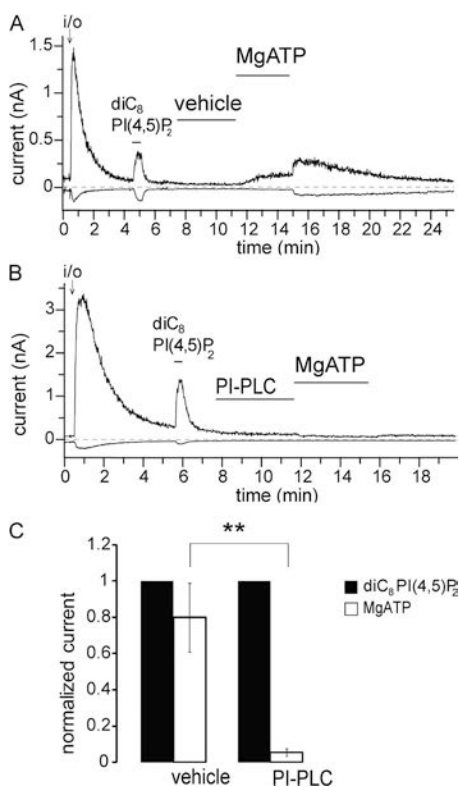


Figure 4. PI-PLC eliminates the effect of MgATP. Excised inside-out patch measurements have been performed on hTRPM3-expressing *Xenopus* oocytes with 100 μM PregS in the patch pipette as described in Materials and methods; data are plotted at 100 and −100 mV. (A and B) Representative traces for the effects of MgATP in the absence and presence of PI-PLC; the applications of 2 mM MgATP, 1 U/ml PI-PLC, and 25 μM diC₈ PI(4,5)P₂ are indicated by the horizontal lines. Vehicle denotes standard bath solution with 0.5% glycerol. (C) Summary of the data for control and PI-PLC-treated patches ($n = 6$). Error bars represent SEM. **, $P < 0.01$.

inhibited. When the holding potential was returned to −100 mV, TRPM3 currents recovered to the same levels as before the depolarizing pulse within ~20 s, similar to data obtained with PI(4,5)P₂-dependent KCNQ channels (Falkenburger et al., 2010). In cells transfected with the C363S mutant of ci-VSP lacking phosphatase activity (Okamura et al., 2009), TRPM3 currents were not significantly different before and after the depolarizing pulse (Fig. 6, B and C).

An alternative approach to ci-VSP is the rapamycin-inducible translocation of a 5'-phosphatase to the plasma membrane, based on the heterodimerization of FKBP12 and the FRB fragment of the mammalian target of rapamycin (Suh et al., 2006; Varnai et al., 2006). Fig. 6 (D–F) shows measurements where the components of the inducible 5'-phosphatase (Varnai et al., 2006) were co-expressed with the mTRPM3α2 in HEK293 cells. Application of rapamycin induced a slowly developing ~80% inhibition in cells expressing the active phosphatase, whereas there was essentially no inhibition in control cells expressing all components of the translocation system, without the phosphatase (Fig. 6, D–F). Rapamycin-induced inhibition was not reversible on the time scale of the experiments, consistent with earlier studies (Suh

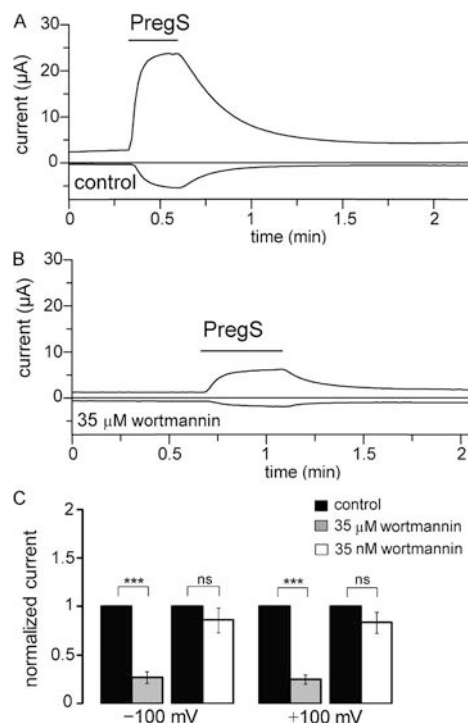


Figure 5. Inhibiting PI4K decreases hTRPM3 current. (A and B) Representative data from two TEVC measurements performed on the same hTRPM3-expressing *Xenopus* oocyte before and after incubation in 35 μM wortmannin for 2 h. Measurements are shown at 100 and −100 mV; the application of 50 μM PregS is shown by horizontal lines. (C) Statistical summary of the data at both positive and negative voltages for the effects of 35 nM ($n = 17$) and 35 μM wortmannin ($n = 14$). Error bars represent SEM. ***, $P < 0.005$.

et al., 2006; Varnai et al., 2006). Rapamycin also induced a small (~20%), but statistically significant inhibition of hTRPM3 in *Xenopus* oocytes expressing the 5'-phosphatase, but not in control oocytes (Fig. S5). This small inhibition is consistent with the lower efficiency of the rapamycin-inducible system in oocytes (Lukacs et al., 2007).

To evaluate the possible contribution of PI(4)P to channel activity, we also tested the effects of rapamycin in HEK cells expressing pseudojanin, an inducible combined 5'- and 4'-phosphatase that reduces both PI(4,5)P₂ and PI(4)P levels (Hammond et al., 2012). Application of rapamycin inhibited TRPM3 currents in these cells (Fig. 7) to a similar extent to that observed in cells expressing the 5'-phosphatase in experiments in Fig. 6 D; see Fig. 7 E for comparison of the time course of inhibition by the different phosphatases. Even though pseudojanin has the same phosphatase domain (INPP5E) as the rapamycin-inducible phosphatase used in Fig. 6, its 5'-phosphatase activity is somewhat lower (Hammond, G. and T. Balla, personal communication), probably because it is a larger construct, also containing the 4'-phosphatase sac1, which may lead to poorer expression. Therefore, we also used a variant of pseudojanin, in which the 4'-phosphatase domain is inactivated with a point mutation (PJ 5'-Ptase). This construct is the

same size as pseudojanin; thus, its 5'-phosphatase activity is expected to be the same. Rapamycin application in the cells expressing the PJ 5'-Ptase inhibited TRPM3 currents significantly less than in cells expressing pseudojanin (Fig. 7, B, D, and E). In control experiments, we used a pseudojanin clone in which both the 4'- and 5'-phosphatases were inactivated (Fig. 7 C). Current levels in these cells also showed a small decrease after application of rapamycin, but the decrease induced by rapamycin was significantly larger both in cells expressing the intact pseudojanin or the PJ 5'-Ptase (Fig. 7 D).

PLC activation inhibits TRPM3 currents

To test whether activation of PLCβ enzymes inhibits TRPM3 current, we coexpressed mTRPM3 channels and human muscarinic M1 receptors (hM1) in HEK cells. We performed these experiments in the presence of extracellular Ca²⁺, which promotes desensitization in many TRP channels (Gordon-Shaag et al., 2008) and also renders PLC activation more efficient upon GPCR activation (Horowitz et al., 2005). PregS-induced currents displayed clear partial desensitization, i.e., decrease in current amplitude in the continuous presence of PregS (Fig. 8). Application of carbachol induced a fast and essentially complete inhibition of PregS-induced currents (Fig. 8).

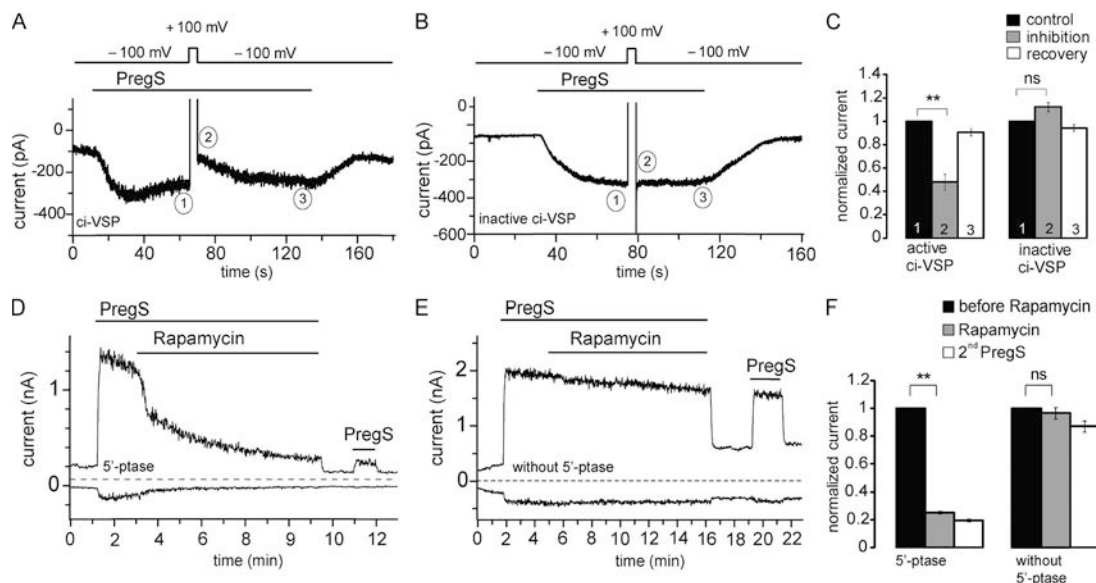


Figure 6. Rapidly inducible 5'-phosphatases inhibit mTRPM3 α 2. (A) Representative trace of mTRPM3 current recorded from a HEK cell transfected with the active ci-VSP at a holding potential of -100 mV followed by short depolarizing pulse of 100 mV to activate the phosphatase. (B) Representative trace from a HEK cell transfected with the phosphatase-inactive mutant of ci-VSP (C363S) using the same voltage protocol as in A. (C) Summary of the inhibition of PregS-induced TRPM3 current plotted by comparing the current at -100 mV before and immediately after the depolarization pulse for the active ($n = 6$) and inactive phosphatases ($n = 5$). (D) Representative measurement in a HEK cell expressing the mTRPM3 and the components of the rapamycin-inducible 5-phosphatase. Measurements were performed using a ramp protocol from -100 to 100 mV, and current amplitudes are plotted at 100 and -100 mV. The applications of 25 μ M PregS and 100 nM rapamycin are indicated by the horizontal lines. (E) Similar experiment as in D in a control cell, expressing TRPM3 and the components of the rapamycin-inducible system without the 5-phosphatase. (F) Statistical summary of the data ($n = 6-7$). Error bars represent SEM. **, $P < 0.01$.

DISCUSSION

TRPM3 is a phosphoinositide-dependent ion channel. Regulation of TRP channels by PI(4,5)P₂ is complex and in some cases controversial. Although the majority of them are positively regulated by PI(4,5)P₂, negative effects of this lipid have also been described on several members of the TRPC and TRPV families, in some cases concurrent with positive effects (reviewed in Rohacs [2014]). The heat- and capsaicin-sensitive TRPV1 is a prime example of these ongoing debates (Cao et al., 2013b; Lukacs et al., 2013; Senning et al., 2014; reviewed in Rohacs [2015]).

These controversies and complexities are not unique to the TRP field, and some of the discrepancies may arise from the differences in the techniques used by different groups (Hilgemann, 2012). Voltage-gated K⁺ (Kv) channels, for example, were suggested to be regulated by PI(4,5)P₂ based on application of phosphoinositide micelles to excised patches (Oliver et al., 2004; Decher et al., 2008), but experiments with inducible phosphatases in the whole-cell configuration suggested no dependence on PI(4,5)P₂ for most Kv channels, with the exception of the Kv7 (KCNQ) family (Kruse et al., 2012).

To avoid inherent problems with relying on one experimental setting, here we used a wide array of approaches both in excised inside-out patches and in the whole-cell configuration. We found that TRPM3 currents show marked rundown in excised patches and channel activity could be restored both by application of natural long acyl chain PI(4,5)P₂ and synthetic diC₈ PI(4,5)P₂. Application of MgATP after rundown also restored channel activity. This effect was eliminated both by inhibiting PI4K enzymes and by removal of phosphatidylinositol

using the bacterial PI-PLC enzyme, demonstrating that MgATP acted via increasing endogenous phosphoinositide levels. In whole-cell patch clamp experiments, channel activity was inhibited by four different inducible phosphoinositide phosphatases, as well as activation of PLC. Overall, we concluded that TRPM3 channels, similarly to other members of the TRPM family, require phosphoinositides for activity.

Quantitative considerations and phosphoinositide specificity
Even though our results clearly point to PI(4,5)P₂ being an important cofactor for TRPM3 activity, some quantitative discrepancies between the results obtained with different approaches require discussion. TRPM3 channels displayed an almost complete rundown in excised patches, indicating a strong dependence on phosphoinositides. Rundown in most cases was relatively fast, indicating low or moderate apparent affinity for PI(4,5)P₂. Consistent with this, the EC₅₀ of ~18 μM for diC₈ PI(4,5)P₂, indicates an intermediate affinity of TRPM3 to PI(4,5)P₂ between high-affinity channels (EC₅₀ < 5 μM), such as Kir2.1 (Du et al., 2004) or TRPV1 (Klein et al., 2008) and low-affinity channels such as KCNQ-s (EC₅₀ > 40 μM; Zhang et al., 2003; Li et al., 2005).

It was calculated that application of ~40 μM diC₈ PI(4,5)P₂ to excised patches results in a mole fraction of 0.01 (1%) of diC₈ PI(4,5)P₂ in the inner leaflet on the plasma membrane, which is considered the physiological concentration there (Collins and Gordon 2013). Based on our dose-response measurements, this physiological level of diC₈ PI(4,5)P₂ (40 μM) induced an ~67% saturation of TRPM3 currents (Fig. 1 F). This is comparable with our AAST PI(4,5)P₂ measurement, where the maximal current induced by this lipid was ~1.6 times

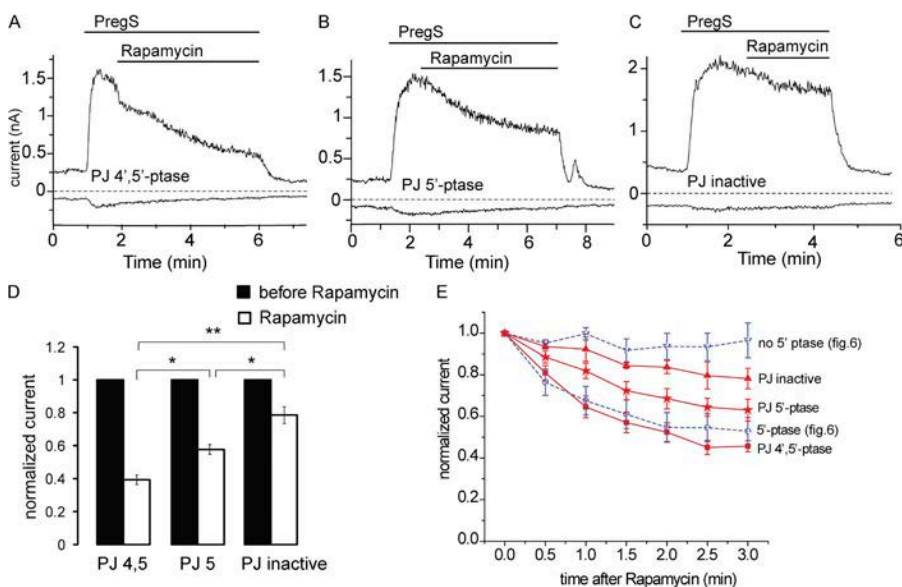


Figure 7. The effects of the rapamycin-inducible 4'- and 5'-phosphatase pseudojanin. (A) Representative measurement in a HEK cell expressing the mTRPM3 and the components of the rapamycin-inducible 4'- and 5'-phosphatase pseudojanin. Measurements were performed using a ramp protocol from -100 to 100 mV, and current amplitudes are plotted at 100 and -100 mV. The applications of 25 μM PregS and 100 nM rapamycin are indicated by the horizontal lines. (B) Similar measurements as in A in a cell transfected with a pseudojanin construct in which the 4'-phosphatase was inactivated. (C) Similar measurements as in A in a cell in which both the 5'- and the 4'-phosphatase domains in pseudojanin were inactivated. (D) Summary of the extent of inhibition at the end of rapamycin application. (E) Time course of inhibition for the three pseudojanin constructs and for the 5'-phosphatase and its control construct from Fig. 6. Error bars represent SEM. *, P < 0.05; **, P < 0.01.

that of the current after excision (Fig. 1 D), which we assume to reflect the effect of endogenous physiological levels of PI(4,5)P₂. Thus, based on the AAST PI(4,5)P₂ measurements, endogenous PI(4,5)P₂ induced ~62% of the maximum effect. Overall, the data with diC₈ and AAST PI(4,5)P₂ indicate that endogenous PI(4,5)P₂ exerts 62–67% saturation of TRPM3 activity, which is overall consistent with a moderate apparent affinity for PI(4,5)P₂.

Given the preference of the channel for PI(4,5)P₂ over PI(4)P, its full dependence on PI(4,5)P₂, and its moderate affinity for the lipid, it is expected that the inducible 5'-phosphatases inhibit the channels robustly and quickly. Inhibition by ci-VSP was incomplete, however, and the effect of the rapamycin-inducible 5'-phosphatase developed slowly. Slow or incomplete inhibition by PI(4,5)P₂ depletion is often associated with high apparent affinity for PI(4,5)P₂, which seems to be at odds with the excised patch data, which indicated low/moderate affinity.

The inducible 5'-phosphatases used in this study in whole-cell patch clamp experiments convert PI(4,5)P₂ into PI(4)P. When the effects of diC₈ phosphoinositides were tested in excised patches, PI(4,5)P₂ clearly activated the channel, but PI(4)P had a negligible effect. The natural AAST PI(4)P was also less effective than AAST PI(4,5)P₂, but it induced a quite substantial activation, especially at positive voltages, where it induced ~60% of the effect evoked by AAST PI(4,5)P₂. The concentration

of PI(4)P is generally thought to be comparable in the plasma membrane with that of PI(4,5)P₂. Thus, it is possible that the contribution of PI(4)P to channel activity accounts for incomplete inhibition by the inducible 5'-phosphatases, especially that the concentration of this lipid is expected to acutely increase after activation of a 5'-phosphatase. To test this possibility, we used the combined 4'- and 5'-phosphatase pseudojanin that depletes both PI(4,5)P₂ and PI(4)P (Hammond et al., 2012). Application of rapamycin in pseudojanin-expressing cells did not induce a faster or more complete inhibition than the 5'-phosphatase used in Fig. 6 (Varnai et al., 2006). As mentioned in Results, however, pseudojanin may have a lower 5'-phosphatase activity than the rapamycin-inducible phosphatase we used first. Therefore, we compared the effect of pseudojanin with its variant, in which the 4'-phosphatase is inactivated (PJ 5'-Ptase). In cells transfected with PJ 5'-Ptase, rapamycin induced a smaller inhibition than in cells with the intact pseudojanin. This suggests that PI(4)P contributes to TRPM3 activity, which may explain the slow and partial inhibition by the 5'-phosphatases in whole-cell patch clamp experiments.

Overall, both our excised patch and whole-cell data demonstrate that PI(4,5)P₂ is a positive cofactor for PregS-induced TRPM3 activity and that PI(4)P may also contribute to supporting channel activity in a cellular context.

Potential physiological relevance

PI(4,5)P₂ is the substrate for PLC enzymes. We found that stimulation of PLCβ via hM1 receptors robustly inhibited TRPM3 activity. The inhibition was faster and more complete than that induced by any of the inducible phosphoinositide phosphatases, raising the possibility that in addition to PI(4,5)P₂ depletion, other Ca²⁺-sensitive factors, such as calmodulin (Holakovska et al., 2012), may also contribute to this inhibition. It also remains to be seen whether endogenous PLC-coupled receptors also inhibit the channel.

In the presence of extracellular Ca²⁺, PregS-induced TRPM3 currents displayed marked desensitization, i.e., reduced currents despite the continuous presence of PregS. Desensitization of several TRP channels, such as TRPM8 (Rohács et al., 2005), TRPV1 (Lukacs et al., 2007), and TRPV2 (Mercado et al., 2010), has been shown to proceed via Ca²⁺-induced activation of PLC and the resulting depletion of PI(4,5)P₂. Because TRPM3 is Ca²⁺ permeable and its activity depends on PI(4,5)P₂, this mechanism is feasible for its desensitization. We indeed found that application of PregS to cells expressing TRPM3 induced activation of PLC, even though to a lesser extent than carbachol (unpublished data).

PI(3,4,5)P₃, the product of PI3K, had a larger effect on TRPM3 than PI(4,5)P₂. The concentration of PI(3,4,5)P₃ in the plasma membrane is thought to be <10% of that of PI(4,5)P₂ even in stimulated cells (Balla, 2013). PI(3,4,5)P₃ stimulates many phosphoinositide-sensitive

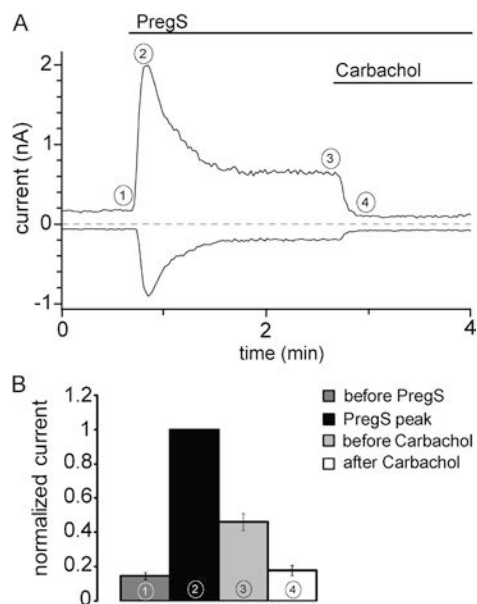


Figure 8. Activation of PLCβ by carbachol inhibits mTRPM3α2 currents. (A) Representative whole-cell patch clamp experiment in a HEK cell expressing mTRPM3α2 and hM1 in the presence of 2 mM extracellular Ca²⁺. The applications of 50 μM PregS and 100 μM carbachol are indicated by the horizontal lines. (B) Summary of data normalized to the peak of the PregS-induced current at the time points indicated. Error bars represent SEM.

channels, usually to a comparable extent with PI(4,5)P₂ (Rohács et al., 2003). Given its much lower concentration, the more abundant PI(4,5)P₂ is likely to override its effect. For TRPM3, however, PI(3,4,5)P₃ had both higher apparent affinity and substantially higher maximal stimulating effect than PI(4,5)P₂. This raises the possibility that PI(3,4,5)P₃ generated by PI3K is capable of further stimulating TRPM3, but testing this hypothesis will require further experiments.

Concluding remarks

Using several different techniques both in excised patches and in whole-cell patch clamp experiments, we demonstrate that PI(4,5)P₂ is an important cofactor of TRPM3. Given that all other members of the TRPM family, with the exception of TRPM1, which is hard to study both in native and recombinant systems, have also been shown to be positively regulated by PI(4,5)P₂, our work establishes TRPM channels as a bona fide PI(4,5)P₂-dependent ion channel family.

The human TRPM3 clone was provided by Christian Harteneck and the mouse TRPM3 α 2 by Drs. Stephan Philipp and Veit Flockerzi. The ci-VSP clone was provided by Dr. Yasushi Okamura, the rapamycin-inducible 5-phosphatase system and compound A1 by Dr. Tamas Balla, and pseudojanin by Dr. Gerald Hammond.

This work was supported by National Institutes of Health grants R01NS055159 and R01GM093290 to T. Rohacs.

The authors declare no competing financial interests.

Sharona E. Gordon served as editor.

Submitted: 26 November 2014

Accepted: 21 May 2015

REFERENCES

Balla, T. 2001. Pharmacology of phosphoinositides, regulators of multiple cellular functions. *Curr. Pharm. Des.* 7:475–507. <http://dx.doi.org/10.2174/1381612013397906>

Balla, T. 2013. Phosphoinositides: tiny lipids with giant impact on cell regulation. *Physiol. Rev.* 93:1019–1137. <http://dx.doi.org/10.1152/physrev.00028.2012>

Bennett, T.M., D.S. Mackay, C.J. Siegfried, and A. Shiels. 2014. Mutation of the melastatin-related cation channel, TRPM3, underlies inherited cataract and glaucoma. *PLoS ONE*. 9:e104000. <http://dx.doi.org/10.1371/journal.pone.0104000>

Bojjireddy, N., J. Botyanski, G. Hammond, D. Creech, R. Peterson, D.C. Kemp, M. Snead, R. Brown, A. Morrison, S. Wilson, et al. 2014. Pharmacological and genetic targeting of the PI4KA enzyme reveals its important role in maintaining plasma membrane phosphatidylinositol 4-phosphate and phosphatidylinositol 4,5-bisphosphate levels. *J. Biol. Chem.* 289:6120–6132. <http://dx.doi.org/10.1074/jbc.M113.531426>

Cao, C., E. Zakharian, I. Borbiro, and T. Rohacs. 2013a. Interplay between calmodulin and phosphatidylinositol 4,5-bisphosphate in Ca²⁺-induced inactivation of transient receptor potential vanilloid 6 channels. *J. Biol. Chem.* 288:5278–5290. <http://dx.doi.org/10.1074/jbc.M112.409482>

Cao, E., J.F. Cordero-Morales, B. Liu, F. Qin, and D. Julius. 2013b. TRPV1 channels are intrinsically heat sensitive and negatively

regulated by phosphoinositide lipids. *Neuron*. 77:667–679. <http://dx.doi.org/10.1016/j.neuron.2012.12.016>

Collins, M.D., and S.E. Gordon. 2013. Short-chain phosphoinositide partitioning into plasma membrane models. *Biophys. J.* 105:2485–2494. <http://dx.doi.org/10.1016/j.bpj.2013.09.035>

Decher, N., T. Gonzalez, A.K. Streit, F.B. Sachse, V. Renigunta, M. Soom, S.H. Heinemann, J. Daut, and M.C. Sanguinetti. 2008. Structural determinants of Kv β 1.3-induced channel inactivation: a hairpin modulated by PIP₂. *EMBO J.* 27:3164–3174. <http://dx.doi.org/10.1038/emboj.2008.231>

Du, X., H. Zhang, C. Lopes, T. Mirshahi, T. Rohacs, and D.E. Logothetis. 2004. Characteristic interactions with phosphatidylinositol 4,5-bisphosphate determine regulation of kir channels by diverse modulators. *J. Biol. Chem.* 279:37271–37281. <http://dx.doi.org/10.1074/jbc.M403413200>

Falkenburger, B.H., J.B. Jensen, and B. Hille. 2010. Kinetics of PIP₂ metabolism and KCNQ2/3 channel regulation studied with a voltage-sensitive phosphatase in living cells. *J. Gen. Physiol.* 135:99–114. <http://dx.doi.org/10.1085/jgp.200910345>

Frühwald, J., J. Camacho Londoño, S. Dembla, S. Mannebach, A. Lis, A. Drews, U. Wissenbach, J. Oberwinkler, and S.E. Philipp. 2012. Alternative splicing of a protein domain indispensable for function of transient receptor potential melastatin 3 (TRPM3) ion channels. *J. Biol. Chem.* 287:36663–36672. <http://dx.doi.org/10.1074/jbc.M112.396663>

Gabriel, T.E., and D. Günzel. 2007. Quantification of Mg²⁺ extrusion and cytosolic Mg²⁺-buffering in *Xenopus* oocytes. *Arch. Biochem. Biophys.* 458:3–15. <http://dx.doi.org/10.1016/j.abb.2006.07.007>

Gordon-Shaag, A., W.N. Zagotta, and S.E. Gordon. 2008. Mechanism of Ca²⁺-dependent desensitization in TRP channels. *Channels (Austin)*. 2:125–129. <http://dx.doi.org/10.4161/chan.2.2.6026>

Grimm, C., R. Kraft, S. Sauerbruch, G. Schultz, and C. Harteneck. 2003. Molecular and functional characterization of the melastatin-related cation channel TRPM3. *J. Biol. Chem.* 278:21493–21501. <http://dx.doi.org/10.1074/jbc.M300945200>

Grubbs, R.D. 2002. Intracellular magnesium and magnesium buffering. *Biometals*. 15:251–259. <http://dx.doi.org/10.1023/A:1016026831789>

Hammond, G.R., M.J. Fischer, K.E. Anderson, J. Holdich, A. Koteci, T. Balla, and R.F. Irvine. 2012. PI4P and PI(4,5)P₂ are essential but independent lipid determinants of membrane identity. *Science*. 337:727–730. <http://dx.doi.org/10.1126/science.1222483>

Hilgemann, D.W. 1997. Cytoplasmic ATP-dependent regulation of ion transporters and channels: mechanisms and messengers. *Annu. Rev. Physiol.* 59:193–220. <http://dx.doi.org/10.1146/annurev.physiol.59.1.193>

Hilgemann, D.W. 2012. Fitting K_v potassium channels into the PIP₂ puzzle: Hille group connects dots between illustrious HH groups. *J. Gen. Physiol.* 140:245–248. <http://dx.doi.org/10.1085/jgp.201210874>

Hilgemann, D.W., and R. Ball. 1996. Regulation of cardiac Na⁺,Ca²⁺ exchange and K_{ATP} potassium channels by PIP₂. *Science*. 273:956–959. <http://dx.doi.org/10.1126/science.273.5277.956>

Holakovska, B., L. Grycova, M. Jirku, M. Sulc, L. Bumba, and J. Teisinger. 2012. Calmodulin and S100A1 protein interact with N terminus of TRPM3 channel. *J. Biol. Chem.* 287:16645–16655. <http://dx.doi.org/10.1074/jbc.M112.350686>

Horowitz, L.F., W. Hirdes, B.C. Suh, D.W. Hilgemann, K. Mackie, and B. Hille. 2005. Phospholipase C in living cells: activation, inhibition, Ca²⁺ requirement, and regulation of M current. *J. Gen. Physiol.* 126:243–262. <http://dx.doi.org/10.1085/jgp.200509309>

Hossain, M.I., H. Iwasaki, Y. Okochi, M. Chahine, S. Higashijima, K. Nagayama, and Y. Okamura. 2008. Enzyme domain affects the movement of the voltage sensor in ascidian and zebrafish

- voltage-sensing phosphatases. *J. Biol. Chem.* 283:18248–18259. <http://dx.doi.org/10.1074/jbc.M706184200>
- Hughes, S., C.A. Potheary, A. Jagannath, R.G. Foster, M.W. Hankins, and S.N. Peirson. 2012. Profound defects in pupillary responses to light in TRPM-channel null mice: a role for TRPM channels in non-image-forming photoreception. *Eur. J. Neurosci.* 35:34–43. <http://dx.doi.org/10.1111/j.1460-9568.2011.07944.x>
- Ingólfsson, H.I., P. Thakur, K.F. Herold, E.A. Hobart, N.B. Ramsey, X. Periole, D.H. de Jong, M. Zwama, D. Yilmaz, K. Hall, et al. 2014. Phytochemicals perturb membranes and promiscuously alter protein function. *ACS Chem. Biol.* 9:1788–1798. <http://dx.doi.org/10.1021/cb500086e>
- Klein, R.M., C.A. Ufret-Vincenty, L. Hua, and S.E. Gordon. 2008. Determinants of molecular specificity in phosphoinositide regulation. Phosphatidylinositol (4,5)-bisphosphate (PI(4,5)P₂) is the endogenous lipid regulating TRPV1. *J. Biol. Chem.* 283:26208–26216. <http://dx.doi.org/10.1074/jbc.M801912200>
- Kruse, M., G.R. Hammond, and B. Hille. 2012. Regulation of voltage-gated potassium channels by PI(4,5)P₂. *J. Gen. Physiol.* 140:189–205. <http://dx.doi.org/10.1085/jgp.201210806>
- Li, Y., N. Gamper, D.W. Hilgemann, and M.S. Shapiro. 2005. Regulation of Kv7 (KCNQ) K⁺ channel open probability by phosphatidylinositol 4,5-bisphosphate. *J. Neurosci.* 25:9825–9835. <http://dx.doi.org/10.1523/JNEUROSCI.2597-05.2005>
- Liu, D., and E.R. Liman. 2003. Intracellular Ca²⁺ and the phospholipid PIP₂ regulate the taste transduction ion channel TRPM5. *Proc. Natl. Acad. Sci. USA.* 100:15160–15165. <http://dx.doi.org/10.1073/pnas.2334159100>
- Logothetis, D.E., V.I. Petrou, M. Zhang, R. Mahajan, X.Y. Meng, S.K. Adney, M. Cui, and L. Baki. 2015. Phosphoinositide control of membrane protein function: a frontier led by studies on ion channels. *Annu. Rev. Physiol.* 77:81–104. <http://dx.doi.org/10.1146/annurev-physiol-021113-170358>
- Lopes, C.M., H. Zhang, T. Rohacs, T. Jin, J. Yang, and D.E. Logothetis. 2002. Alterations in conserved Kir channel-PIP₂ interactions underlie channelopathies. *Neuron.* 34:933–944. [http://dx.doi.org/10.1016/S0896-6273\(02\)00725-0](http://dx.doi.org/10.1016/S0896-6273(02)00725-0)
- Lukacs, V., B. Thyagarajan, P. Varnai, A. Balla, T. Balla, and T. Rohacs. 2007. Dual regulation of TRPV1 by phosphoinositides. *J. Neurosci.* 27:7070–7080. <http://dx.doi.org/10.1523/JNEUROSCI.1866-07.2007>
- Lukacs, V., J.M. Rives, X. Sun, E. Zakharian, and T. Rohacs. 2013. Promiscuous activation of transient receptor potential vanilloid 1 (TRPV1) channels by negatively charged intracellular lipids: the key role of endogenous phosphoinositides in maintaining channel activity. *J. Biol. Chem.* 288:35003–35013. <http://dx.doi.org/10.1074/jbc.M113.520288>
- Mercado, J., A. Gordon-Shaag, W.N. Zagotta, and S.E. Gordon. 2010. Ca²⁺-dependent desensitization of TRPV2 channels is mediated by hydrolysis of phosphatidylinositol 4,5-bisphosphate. *J. Neurosci.* 30:13338–13347. <http://dx.doi.org/10.1523/JNEUROSCI.2108-10.2010>
- Nilius, B., F. Mahieu, J. Prenen, A. Janssens, G. Owsianik, R. Vennekens, and T. Voets. 2006. The Ca²⁺-activated cation channel TRPM4 is regulated by phosphatidylinositol 4,5-bisphosphate. *EMBO J.* 25:467–478. <http://dx.doi.org/10.1038/sj.emboj.7600963>
- Oberwinkler, J., and S.E. Philipp. 2014. TRPM3. *Handbook Exp. Pharmacol.* 222:427–459.
- Oberwinkler, J., A. Lis, K.M. Giehl, V. Flockerzi, and S.E. Philipp. 2005. Alternative splicing switches the divalent cation selectivity of TRPM3 channels. *J. Biol. Chem.* 280:22540–22548. <http://dx.doi.org/10.1074/jbc.M503092200>
- Okamura, Y., Y. Murata, and H. Iwasaki. 2009. Voltage-sensing phosphatase: actions and potentials. *J. Physiol.* 587:513–520. <http://dx.doi.org/10.1113/jphysiol.2008.163097>
- Oliver, D., C.C. Lien, M. Soom, T. Baukowitz, P. Jonas, and B. Fakler. 2004. Functional conversion between A-type and delayed rectifier K⁺ channels by membrane lipids. *Science.* 304:265–270. <http://dx.doi.org/10.1126/science.1094113>
- Rohacs, T. 2013. Recording macroscopic currents in large patches from *Xenopus* oocytes. *Methods Mol. Biol.* 998:119–131. http://dx.doi.org/10.1007/978-1-62703-351-0_9
- Rohacs, T. 2014. Phosphoinositide regulation of TRP channels. *Handbook Exp. Pharmacol.* 223:1143–1176. http://dx.doi.org/10.1007/978-3-319-05161-1_18
- Rohacs, T. 2015. Phosphoinositide regulation of TRPV1 revisited. *Pflugers Arch.* In press. <http://dx.doi.org/10.1007/s00424-015-1695-3>
- Rohács, T., C. Lopes, T. Mirshahi, T. Jin, H. Zhang, and D.E. Logothetis. 2002. Assaying phosphatidylinositol bisphosphate regulation of potassium channels. *Methods Enzymol.* 345:71–92.
- Rohács, T., C.M. Lopes, T. Jin, P.P. Ramdya, Z. Molnár, and D.E. Logothetis. 2003. Specificity of activation by phosphoinositides determines lipid regulation of Kir channels. *Proc. Natl. Acad. Sci. USA.* 100:745–750. <http://dx.doi.org/10.1073/pnas.0236364100>
- Rohács, T., C.M. Lopes, I. Michailidis, and D.E. Logothetis. 2005. PI(4,5)P₂ regulates the activation and desensitization of TRPM8 channels through the TRP domain. *Nat. Neurosci.* 8:626–634. <http://dx.doi.org/10.1038/nn1451>
- Runnels, L.W., L. Yue, and D.E. Clapham. 2002. The TRPM7 channel is inactivated by PIP₂ hydrolysis. *Nat. Cell Biol.* 4:329–336.
- Senning, E.N., M.D. Collins, A. Stratiievska, C.A. Ufret-Vincenty, and S.E. Gordon. 2014. Regulation of TRPV1 ion channel by phosphoinositide (4,5)-bisphosphate: the role of membrane asymmetry. *J. Biol. Chem.* 289:10999–11006. <http://dx.doi.org/10.1074/jbc.M114.553180>
- Stein, A.T., C.A. Ufret-Vincenty, L. Hua, L.F. Santana, and S.E. Gordon. 2006. Phosphoinositide 3-kinase binds to TRPV1 and mediates NGF-stimulated TRPV1 trafficking to the plasma membrane. *J. Gen. Physiol.* 128:509–522. <http://dx.doi.org/10.1085/jgp.200609576>
- Suh, B.C., and B. Hille. 2008. PIP₂ is a necessary cofactor for ion channel function: how and why? *Annu. Rev. Biophys.* 37:175–195. <http://dx.doi.org/10.1146/annurev.biophys.37.032807.125859>
- Suh, B.C., T. Inoue, T. Meyer, and B. Hille. 2006. Rapid chemically induced changes of PtdIns(4,5)P₂ gate KCNQ ion channels. *Science.* 314:1454–1457. <http://dx.doi.org/10.1126/science.1131163>
- Sui, J.L., J. Petit-Jacques, and D.E. Logothetis. 1998. Activation of the atrial K_{ACh} channel by the βγ subunits of G proteins or intracellular Na⁺ ions depends on the presence of phosphatidylinositol phosphates. *Proc. Natl. Acad. Sci. USA.* 95:1307–1312. <http://dx.doi.org/10.1073/pnas.95.3.1307>
- Thiel, G., I. Müller, and O.G. Rössler. 2013. Signal transduction via TRPM3 channels in pancreatic β-cells. *J. Mol. Endocrinol.* 50:R75–R83. <http://dx.doi.org/10.1530/JME-12-0237>
- Tóth, B., and L. Csanády. 2012. Pore collapse underlies irreversible inactivation of TRPM2 cation channel currents. *Proc. Natl. Acad. Sci. USA.* 109:13440–13445. <http://dx.doi.org/10.1073/pnas.1204702109>
- Ufret-Vincenty, C.A., R.M. Klein, L. Hua, J. Angueyra, and S.E. Gordon. 2011. Localization of the PIP₂ sensor of TRPV1 ion channels. *J. Biol. Chem.* 286:9688–9698. <http://dx.doi.org/10.1074/jbc.M110.192526>
- Varnai, P., B. Thyagarajan, T. Rohacs, and T. Balla. 2006. Rapidly inducible changes in phosphatidylinositol 4,5-bisphosphate levels influence multiple regulatory functions of the lipid in intact living cells. *J. Cell Biol.* 175:377–382. <http://dx.doi.org/10.1083/jcb.200607116>
- Vriens, J., G. Owsianik, T. Hofmann, S.E. Philipp, J. Stab, X. Chen, M. Benoit, F. Xue, A. Janssens, S. Kerselaers, et al. 2011.

- TRPM3 is a nociceptor channel involved in the detection of noxious heat. *Neuron*. 70:482–494. <http://dx.doi.org/10.1016/j.neuron.2011.02.051>
- Wagner, T.F., S. Loch, S. Lambert, I. Straub, S. Mannebach, I. Mathar, M. Düfer, A. Lis, V. Flockerzi, S.E. Philipp, and J. Oberwinkler. 2008. Transient receptor potential M3 channels are ionotropic steroid receptors in pancreatic beta cells. *Nat. Cell Biol.* 10:1421–1430. <http://dx.doi.org/10.1038/ncb1801>
- Wu, L.J., T.B. Sweet, and D.E. Clapham. 2010. International Union of Basic and Clinical Pharmacology. LXXVI. Current progress in the mammalian TRP ion channel family. *Pharmacol. Rev.* 62:381–404. <http://dx.doi.org/10.1124/pr.110.002725>
- Xie, J., B. Sun, J. Du, W. Yang, H.C. Chen, J.D. Overton, L.W. Runnels, and L. Yue. 2011. Phosphatidylinositol 4,5-bisphosphate (PIP₂) controls magnesium gatekeeper TRPM6 activity. *Sci. Rep.* 1:146. <http://dx.doi.org/10.1038/srep00146>
- Zakharian, E., C. Cao, and T. Rohacs. 2011. Intracellular ATP supports TRPV6 activity via lipid kinases and the generation of PtdIns(4,5)P₂. *FASEB J.* 25:3915–3928. <http://dx.doi.org/10.1096/fj.11-184630>
- Zhang, H., L.C. Craciun, T. Mirshahi, T. Rohács, C.M. Lopes, T. Jin, and D.E. Logothetis. 2003. PIP₂ activates KCNQ channels, and its hydrolysis underlies receptor-mediated inhibition of M currents. *Neuron*. 37:963–975. [http://dx.doi.org/10.1016/S0896-6273\(03\)00125-9](http://dx.doi.org/10.1016/S0896-6273(03)00125-9)